Phase-sensitive Kerr nonlinearity for closed-loop quantum systems

H. R. Hamedi* and G. Juzeliūnas†

Institute of Theoretical Physics and Astronomy, Vilnius University, A. Goštauto 12, Vilnius LT-01108, Lithuania

(Received 10 December 2014; revised manuscript received 28 March 2015; published 14 May 2015)

The third-order susceptibility is investigated in a five-level atomic system in which the laser beams couple the ground state to a four-level closed-loop system. It is found that under the condition of the multiphoton resonance, one can enhance the Kerr nonlinearity of such a medium by properly adjusting the amplitudes and phases of the applied fields. In this case, the linear and nonlinear absorption reduce considerably in a region with a positive group velocity. It is demonstrated that the third-order susceptibility is very sensitive to the relative phase of the applied fields. An analytical model is presented to elucidate such phase control of the Kerr nonlinearity. A comparison is also made between the Kerr-nonlinear indices for the five-, four-, and three-level systems. It is realized that the magnitude of the Kerr nonlinearity for the five-level system is larger than that of the three- and four-level counterparts. Finally, it is shown that effect of Doppler broadening can lead to an enhanced Kerr nonlinearity while maintaining linear and nonlinear absorption.

DOI: 10.1103/PhysRevA.91.053823 PACS number(s): 42.50.Gy, 42.65.Pc

I. INTRODUCTION

Third-order optical nonlinearity is encountered in any material regardless of its spatial symmetry [1]. Since all even-order nonlinearities are identically equal to zero in central symmetric materials, the third-order nonlinearity represents the lowest-order nonvanishing nonlinear optical susceptibility. Kerr nonlinearity, which is proportional to the refractive part of the third-order susceptibility, plays an important role in optical data processing because it can be used to control a signal of light by means of another light beam. The optical Kerr nonlinearity also allows propagation of ultrashort soliton-type pulses without spreading [2]. It is desirable to have large third-order nonlinear susceptibilities under conditions of low light power and high sensitivities [3,4] since it can be used for realization of single-photon nonlinear devices. This requires that the linear susceptibilities should be as small as possible compared to the nonlinear ones. For many years, experimental research on quantum nonlinear optics has been limited because of a weak nonlinear response of even the best materials.

Electromagnetically induced transparency (EIT) [5,6] has opened a possibility to achieve large nonlinearities [7]. Electromagnetically induced transparency also has many notable applications in quantum and nonlinear optics such as multiwave mixing [8–10], optical bistability [11,12], optical solitons [13–17], and Kerr nonlinearity [18]. Many proposals have been suggested both theoretically and experimentally for achieving enhanced Kerr nonlinearity accompanied by negligible absorption in three- and four-level atomic systems [19–26]. Wang *et al.* [19] studied experimentally the enhanced Kerr nonlinear coefficient in a three-level Λ-type atomic system for various powers of the coupling beam. They showed that the Kerr nonlinear coefficient behaves very differently in the regions of strong- and weak-coupling power and changes its sign when the coupling or the probe frequency detuning changes a sign. It was found that the Kerr nonlinear index can be greatly enhanced (compared to that in a two-level atomic system) due to the atomic coherence in the three-level atomic system. Niu and Gong [20] investigated theoretically the effect of spontaneously generated coherence on the Kerr nonlinearity of three-level systems of the Λ-, ladder-, and V-shape types. They found that with the spontaneously generated coherence the Kerr nonlinearity can be clearly enhanced. In the Λ- and ladder-type systems, the maximum Kerr nonlinearity increases and at the same time enters the EIT window as the spontaneously generated coherence gets larger. As for the V-type system, the absorption property is significantly modified and thus an enhancement of the Kerr nonlinearity without absorption occurs for certain probe detuning.

In another study, Niu *et al.* [21] proposed a scheme for a giant enhancement of the Kerr nonlinearity in a four-level system with double dark resonances. They showed that the Kerr nonlinearity can be enhanced by several orders of magnitude (compared to the one generated in a single-dark-resonance system) accompanied by a vanishing linear absorption. This dramatic enhancement was attributed to the interaction of dark resonances [21]. By using an efficient state-preparation technique for the ^{87}Rb D_1 line, Hun *et al.* demonstrated that an ideal four-level tripod-type atomic system can be formed that generates a large cross-Kerr-nonlinearity via interacting dark states in this system [24].

Recently, the self-Kerr-nonlinearity of a four-level N-type atomic system was investigated near atomic resonance by Sheng *et al.* [25]. They showed that the self-Kerr-nonlinear coefficient of the probe field can be greatly enhanced by properly adjusting the switching laser intensity. In addition, they compared both experimentally and theoretically the self-Kerr-nonlinear coefficients for different atomic energy-level configurations of the two-, three-, and four-level cases. In particular, they found that the magnitude of the self-Kerr-nonlinear index for the four-level N-type atomic has the same value as that for the three-level system. All of these studies have dealt with the three- and four-level atomic systems. More recently, Khoa *et al.* [26] investigated theoretically the possibility of obtaining an enhanced self-Kerr-nonlinearity under the EIT condition for a five-level cascade system. They also made a comparison between the behavior of self-Kerr-nonlinearity for such a five-level atomic system with that of

*hamid.r.hamedi@gmail.com
†gediminas.juzeliunas@tfai.vu.lt

four- and three-level cascade systems and observed the same magnitude of the self-Kerr-nonlinear coefficient among the three systems.

Due to its possible application in all-optical switching, quantum information processing, and novel photonic devices, especially at the few-photon level [27–29], it is expected that more experimental studies on this subject will be carried out. Thus, practical schemes are needed to achieve the Kerr-nonlinearity enhancement.

In this paper a five-level atomic system is proposed that was first introduced by Kobrak and Rice to establish a complete population transfer [30,31] to a single target of a degenerate pair of states [32]. The Kobrak-Rice five-level (KR5) system was also employed to show advantages of the coherent control of atomic or molecular processes [33]. Moreover, by using intense laser fields, a new quantum measurement has been introduced in the KR5 system [34]. Dispersion and absorption and optical bistability of this configuration have also been investigated [35,36]. However, the third-order nonlinear susceptibility for this medium has motivated our study.

Here we show that an enhanced Kerr nonlinearity with a reduced absorption can be obtained under the condition of slow light propagation. We find that the Kerr nonlinearity is very sensitive to the relative phase of the applied fields and explore the influence of the relative phase on the linear and nonlinear optical properties of the medium. In particular, it is shown that under the condition of the multiphoton resonance, one can enhance the Kerr nonlinearity of such a medium by properly adjusting the amplitudes and phases of the applied fields. In this case, the linear and nonlinear absorption are reduced remarkably in the region of the subluminal light propagation. Also, we make a comparison between the Kerr-nonlinear indices for this five- level system with that of the existing four- and three-level atomic systems. We find that the magnitude of the Kerr nonlinearity of the KR5 system is larger than that of four- and three-level systems. The influence of the Doppler broadening on the Kerr nonlinearity is also studied. We find considerable changes in shape for the Kerr nonlinearity for a small Doppler width below the natural linewidth of the probe transition for which the linear susceptibility behaves very similarly in shape to the nonbroadened case. In addition, it is observed that the effect of the Doppler broadening can lead to a giant Kerr nonlinearity.

The main advantages of applying the considered five-level system over the atomic schemes proposed in Refs. [25,26] are as follows. First, different from the atomic schemes explored in those works, in the present study the higher orders of nonlinearity are achieved by increasing the number of atomic levels. This can be used for construction of nonclassical states of light as well as coherent processing of quantum information. Second, due to the closed-loop structure interacting with the ground level, this medium is phase sensitive. This phase-sensitive property provides an extra degree of freedom for controlling the Kerr-nonlinear index, a feature that was absent in Refs. [25,26]. This allows us to present an analytical model to elucidate the phase control of the Kerr nonlinearity. Third, in addition to the steady-state nonlinear susceptibilities, in this paper the transient switching of the Kerr nonlinearity is also investigated, which may provide results helpful for the realization of fast optical nonlinearities and optically controlled optical devices. Finally, the effect of the Doppler-broadening effect on the Kerr nonlinearity is studied. In particular, it is found that the effect of the Doppler broadening can lead to a giant Kerr nonlinearity. This is an advantage of this type of Kerr-nonlinearity enhancement over EIT technique (see, for instance, Refs. [19,21,23–26]) because one does not need very-strong-coupling laser fields. A disadvantage of this method is that the linear and nonlinear absorption is not eliminated.

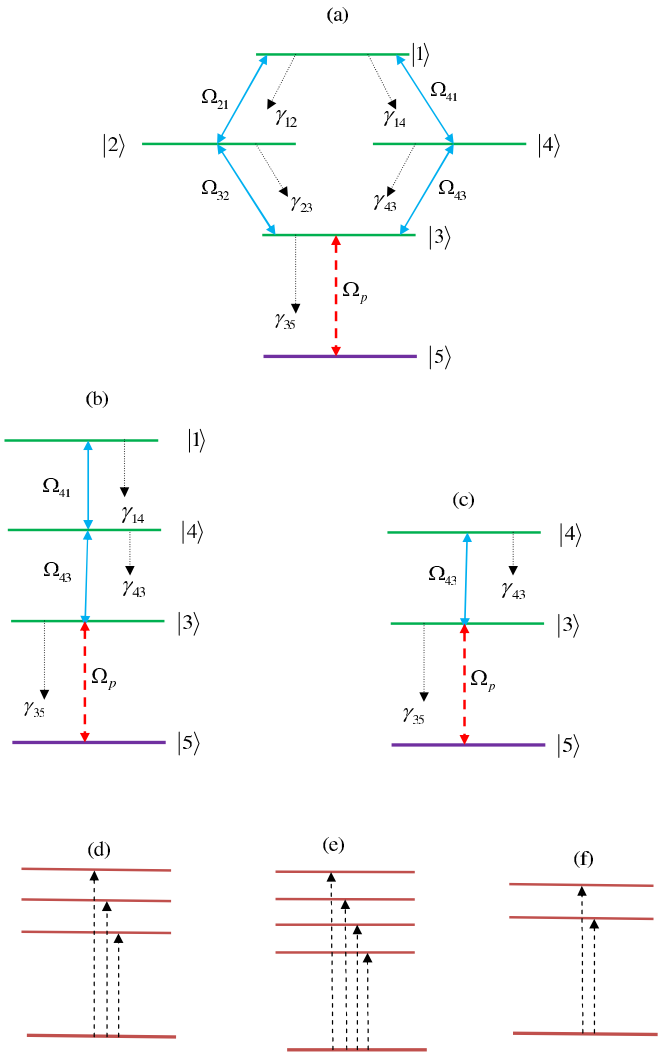

FIG. 1. (Color online) Schematic diagram of the (a) five-, (b) four-, and (c) three-level quantum systems. (d)–(f) General atom-field states in the new basis.

II. MODEL AND EQUATIONS

We shall consider the KR5 quantum system shown in Fig. 1(a). The system has an excited state $|1\rangle$, two nondegenerate metastable lower states $|3\rangle$and $|5\rangle$, and two intermediate degenerate states $|4\rangle$and $|2\rangle$. The Rabi frequencies Ω_{43}, Ω_{32}, Ω_{41}, and Ω_{21} couple a pair of atomic internal states $|1\rangle$ and $|3\rangle$ to another pair of states $|4\rangle$ and $|2\rangle$ in all possible ways

to form a closed-loop scheme of the atom-light interaction, as depicted in Fig. 1(a). Note that such a scheme is equivalent to a consequently coupled cyclic chain of four states $|1\rangle$, $|2\rangle$, $|3\rangle$, and$|4\rangle$, making a diamond-shape closed-loop system. An additional tunable coherent probe field with Rabi frequency Ω_p is applied to the dipole-allowed optical transition $|5\rangle \leftrightarrow |3\rangle$, which couples the diamond-shape system to the ground (or metastable) state $|5\rangle$. The spontaneous decay rates of the upper level $|i\rangle$ to the lower level $|k\rangle$ are denoted by $2\gamma_{ik}$. The spontaneous decays from the excited state $|1\rangle$to the lower levels $|3\rangle$ and $|5\rangle$ are ignored. The total Hamiltonian of the system is given by

$$H_{5\text{-level}} = -\hbar(\Omega_p\,|3\rangle\langle 5| + \Omega_{41}\,|1\rangle\, e^{i\phi}\,\langle 4| + \Omega_{21}\,|2\rangle\langle 1| + \Omega_{32}\,|3\rangle\langle 2| + \Omega_{43}\,|4\rangle\langle 3|) + \text{H.c.}, \tag{1}$$

where $\phi = \phi_{41} + \phi_{43} - \phi_{32} - \phi_{21}$ is the relative phase accumulated after completing a cyclic loop and ϕ_{ij} denotes the phase of the laser field that is applied to the transition $|i\rangle \leftrightarrow |j\rangle$. The equation of the motion for the density operator describing an atomic system can be written as

$$\dot{\rho} = -\frac{i}{\hbar}[H_{5\text{-level}}, \rho] + L_\rho, \tag{2}$$

where L_ρ represents decay rates for the system. Applying the rotating-wave approximation, the equation of motion (2) reduces to

$$\dot{\rho}_{11} = -2(\gamma_{14}+\gamma_{12})\rho_{11} + i\Omega_{41}e^{i\phi}\rho_{41} - i\Omega_{41}^* e^{-i\phi}\rho_{14} - i\Omega_{21}^*\rho_{12} + i\Omega_{21}\rho_{21}, \tag{3a}$$

$$\dot{\rho}_{22} = 2\gamma_{12}\rho_{11} - 2\gamma_{23}\rho_{22} + i\Omega_{32}\rho_{32} - i\Omega_{32}^*\rho_{23} + i\Omega_{21}^*\rho_{12} - i\Omega_{21}\rho_{21}, \tag{3b}$$

$$\dot{\rho}_{33} = 2\gamma_{43}\rho_{44} + 2\gamma_{23}\rho_{22} - 2\gamma_{35}\rho_{33} - i\Omega_{43}\rho_{34} + i\Omega_{43}^*\rho_{43} - i\Omega_{32}\rho_{32} + i\Omega_{32}^*\rho_{23} - i\Omega_p^*\rho_{35} + i\Omega_p\rho_{53}, \tag{3c}$$

$$\dot{\rho}_{44} = 2\gamma_{14}\rho_{11} - 2\gamma_{43}\rho_{44} + i\Omega_{43}\rho_{34} - i\Omega_{43}^*\rho_{43} + i\Omega_{41}^* e^{-i\phi}\rho_{14} - i\Omega_{41}e^{i\phi}\rho_{41}, \tag{3d}$$

$$\dot{\rho}_{41} = \Im_1\rho_{41} + i\Omega_{41}^* e^{-i\phi}(\rho_{11} - \rho_{44}) + i\Omega_{43}\rho_{31} - i\Omega_{21}^*\rho_{42}, \tag{3e}$$

$$\dot{\rho}_{42} = \Im_2\rho_{42} + i\Omega_{43}\rho_{32} + i\Omega_{41}^* e^{-i\phi}\rho_{12} - i\Omega_{32}^*\rho_{43} - i\Omega_{21}\rho_{41}, \tag{3f}$$

$$\dot{\rho}_{43} = \Im_3\rho_{43} + i\Omega_{43}(\rho_{33} - \rho_{44}) + i\Omega_{41}^* e^{-i\phi}\rho_{13} - i\Omega_{32}\rho_{42} - i\Omega_p^*\rho_{45}, \tag{3g}$$

$$\dot{\rho}_{45} = \Im_4\rho_{45} + i\Omega_{41}^* e^{-i\phi}\rho_{15} + i\Omega_{43}\rho_{35} - i\Omega_p\rho_{43}, \tag{3h}$$

$$\dot{\rho}_{21} = \Im_5\rho_{21} + i\Omega_{32}\rho_{31} + i\Omega_{21}^*(\rho_{11} - \rho_{22}) - i\Omega_{41}^* e^{-i\phi}\rho_{24}, \tag{3i}$$

$$\dot{\rho}_{23} = \Im_6\rho_{23} + i\Omega_{32}\rho_{33} - i\Omega_{32}^*\rho_{22} + i\Omega_{21}^*\rho_{13} - i\Omega_{43}\rho_{24} - i\Omega_p^*\rho_{25}, \tag{3j}$$

$$\dot{\rho}_{25} = \Im_7\rho_{25} + i\Omega_{32}\rho_{35} + i\Omega_{21}^*\rho_{15} - i\Omega_p\rho_{23}, \tag{3k}$$

$$\dot{\rho}_{31} = \Im_8\rho_{31} + i\Omega_{32}^*\rho_{21} + i\Omega_{43}^*\rho_{41} + i\Omega_p\rho_{51} - i\Omega_{41}^* e^{-i\phi}\rho_{34} - i\Omega_{21}^*\rho_{32}, \tag{3l}$$

$$\dot{\rho}_{35} = \Im_9\rho_{35} + i\Omega_{32}^*\rho_{25} + i\Omega_{43}^*\rho_{45} + i\Omega_p(\rho_{55} - \rho_{33}), \tag{3m}$$

$$\dot{\rho}_{15} = \Im_{10}\rho_{15} + i\Omega_{41}e^{i\phi}\rho_{45} + i\Omega_{21}\rho_{25} - i\Omega_p\rho_{13}, \tag{3n}$$

$$\rho_{11} + \rho_{22} + \rho_{33} + \rho_{44} + \rho_{55} = 1, \tag{3o}$$

where $\Im_1 = -[i\Delta_{14} + (\gamma_{43}+\gamma_{14}+\gamma_{12})]$, $\Im_2 = i(\Delta_{12}-\Delta_{14}) - (\gamma_{43}+\gamma_{23})$, $\Im_3 = i\Delta_{43} - \gamma_{43} - \gamma_{35}$, $\Im_4 = -[i(\Delta_{43}+\Delta_p) - \gamma_{43}]$, $\Im_5 = -[i\Delta_{12} + (\gamma_{23}+\gamma_{14}+\gamma_{12})]$, $\Im_6 = i(\Delta_{12}-\Delta) - \gamma_{23}$, $\Im_7 = i(\Delta_{23}-\Delta+\Delta_p) - \gamma_{23}$, $\Im_8 = -[i(\Delta_{14}+\Delta_{43}) + (\gamma_{14}+\gamma_{12})]$, $\Im_9 = -(\gamma_{35} - i\Delta_p)$, and $\Im_{10} = i(\Delta_{14}+\Delta_{43}+\Delta_p) - (\gamma_{14}+\gamma_{12})$. Here $\Delta_{43} = \omega_4 - \omega_{43}$, $\Delta_{23} = \omega_2 - \omega_{23}$, $\Delta_{14} = \omega_3 - \omega_{14}$, $\Delta_{12} = \omega_1 - \omega_{12}$, and $\Delta_p = \omega_p - \omega_{35}$ are the one-photon resonance detuning for the transitions $|4\rangle \leftrightarrow |3\rangle$, $|2\rangle \leftrightarrow |3\rangle$, $|1\rangle \leftrightarrow |4\rangle$, $|2\rangle \leftrightarrow |1\rangle$, and $|3\rangle \leftrightarrow |5\rangle$, respectively. The parameter $\Delta = \Delta_{12} - \Delta_{14} + \Delta_{23} - \Delta_{43}$ defines the frequency of the multiphoton detuning and ω_i shows the central frequency of the corresponding laser field.

In order to derive the linear and nonlinear susceptibilities, we need to solve the density-matrix equations for the steady state. Under the weak-field approximation one can apply the perturbation approach

$$\rho_{ij} = \rho_{ij}^{(0)} + \rho_{ij}^{(1)} + \rho_{ij}^{(2)} + \rho_{ij}^{(3)} + \cdots, \tag{4}$$

where the constituting terms $\rho_{ij}^{(0)}$, $\rho_{ij}^{(1)}$, $\rho_{ij}^{(2)}$, and $\rho_{ij}^{(3)}$are of the zeroth, first, second, and third order in the probe field Ω_p. Due to the assumption $\Omega_p \ll \Omega_{43}, \Omega_{32}, \Omega_{41}, \Omega_{21}$, the zeroth-order solution is $\rho_{55}^{(0)} = 1$, with other elements being zero ($\rho_{ij}^{(0)} = 0$, where $i, j \neq 5$). Using this condition and substituting Eq. (4) into Eq. (3), the equations of motion for the first-order density-matrix elements read

$$\dot{\rho}_{35}^{(1)} = \Im_9\rho_{35}^{(1)} + i\Omega_{32}^*\rho_{25}^{(1)} + i\Omega_{43}^*\rho_{45}^{(1)} + i\Omega_p, \tag{5a}$$

$$\dot{\rho}_{25}^{(1)} = \Im_7\rho_{25}^{(1)} + i\Omega_{32}\rho_{35}^{(1)} + i\Omega_{21}^*\rho_{15}^{(1)} - i\Omega_p\rho_{23}^{(1)}, \tag{5b}$$

$$\dot{\rho}_{45}^{(1)} = \Im_4\rho_{45}^{(1)} + i\Omega_{41}^{*}e^{-i\phi}\rho_{15}^{(1)} + i\Omega_{43}\rho_{35}^{(1)}, \tag{5c}$$

$$\dot{\rho}_{15}^{(1)} = \Im_{10}\rho_{15}^{(1)} + i\Omega_{41}e^{i\phi}\rho_{45}^{(1)} + i\Omega_{21}\rho_{25}^{(1)}. \tag{5d}$$

Similarly, the equations of motion for the third-order density-matrix element read

$$\dot{\rho}_{35}^{(3)} = \Im_9\rho_{35}^{(3)} + i\Omega_{32}^{*}\rho_{25}^{(3)} + i\Omega_{43}^{*}\rho_{45}^{(3)} + i\Omega_p\big(\rho_{55}^{(2)} - \rho_{33}^{(2)}\big), \tag{6a}$$

$$\dot{\rho}_{25}^{(3)} = \Im_7\rho_{25}^{(3)} + i\Omega_{32}\rho_{35}^{(3)} + i\Omega_{21}^{*}\rho_{15}^{(3)} - i\Omega_p\rho_{23}^{(2)}, \tag{6b}$$

$$\dot{\rho}_{45}^{(3)} = \Im_4\rho_{45}^{(3)} + i\Omega_{41}^{*}e^{-i\phi}\rho_{15}^{(3)} + i\Omega_{43}\rho_{35}^{(3)} - i\Omega_p\rho_{43}^{(2)}, \tag{6c}$$

$$\dot{\rho}_{15}^{(3)} = \Im_{10}\rho_{15}^{(3)} + i\Omega_{41}e^{i\phi}\rho_{45}^{(3)} + i\Omega_{21}\rho_{25}^{(3)} - i\Omega_p\rho_{13}^{(2)}. \tag{6d}$$

After some algebraic calculations, we obtain the following the off-diagonal density-matrix elements $\rho_{35}^{(1)}$ and $\rho_{35}^{(3)}$ corresponding to Ω_p:

$$\rho_{35}^{(1)} = i\Omega_p\big(\Omega_{21}^2\Im_4 - \Omega_{41}^2\Im_7 + \Im_4\Im_7\Im_{10}\big)/\Re \tag{7}$$

and

$$\begin{aligned}\rho_{35}^{(3)} = {}& \Omega_p\rho_{43}^{(2)}\big(\Omega_{41}\Omega_{21}\Omega_{32}e^{i\phi} - \Omega_{43}\Omega_{21}^2 - \Omega_{43}\Im_7\Im_{10}\big)/\Re + \Omega_p\rho_{23}^{(2)}\big(i\Omega_{32}\Im_4\Im_{10} - \Omega_{41}^2\Omega_{32} + \Omega_{41}\Omega_{21}\Omega_{43}e^{-i\phi}\big)/\Re \\ & + i\rho_{55}^{(2)}\Omega_p\big(\Omega_{21}^2\Im_4 - \Omega_{41}^2\Im_7 + \Im_7\Im_4\Im_{10}\big)/\Re - i\rho_{33}^{(2)}\Omega_p\big(\Omega_{21}^2\Im_4 - \Omega_{41}^2\Im_7 + \Im_7\Im_4\Im_{10}\big)/\Re \\ & - i\rho_{13}^{(2)}\Omega_p\big(\Omega_{41}\Omega_{43}\Im_7e^{-i\phi} - \Omega_{21}\Omega_{23}\Im_4\big)/\Re,\end{aligned} \tag{8}$$

where

$$\begin{aligned}\Re = {}& \Im_4\Im_{10}\Omega_{32}^2 - \Omega_{41}^2\Omega_{32}^2 - \Omega_{43}^2\Omega_{21}^2 - \Im_7\Im_{10}\Omega_{43}^2 - \Im_4\Im_9\Omega_{21}^2 + \Im_7\Im_9\Omega_{41}^2 - \Im_4\Im_7\Im_9\Im_{10} \\ & + 2\Omega_{41}\Omega_{32}\Omega_{43}\Omega_{21}\cos\phi.\end{aligned} \tag{9}$$

Note that the second-order nonlinearity of Eq. (8) is solved to obtain $\rho_{ij}^{(2)}$, giving the steady-state results

$$\rho_{41}^{(2)} = \big[i\Omega_{41}^{*}e^{-i\phi}\big(\rho_{44}^{(2)} - \rho_{11}^{(2)}\big) - i\Omega_{43}\rho_{31}^{(2)} + i\Omega_{21}^{*}\rho_{12}^{(2)}\big]/\Im_1, \tag{10a}$$

$$\rho_{42}^{(2)} = \big(-i\Omega_{43}\rho_{32}^{(2)} - i\Omega_{41}^{*}e^{-i\phi}\rho_{12}^{(2)} + i\Omega_{32}^{*}\rho_{43}^{(2)} + i\Omega_{21}\rho_{14}^{(2)}\big)/\Im_2, \tag{10b}$$

$$\rho_{43}^{(2)} = \big[i\Omega_{43}\big(\rho_{44}^{(2)} - \rho_{33}^{(2)}\big) - i\Omega_{41}^{*}e^{-i\phi}\rho_{13}^{(2)} + i\Omega_{32}\rho_{42}^{(2)} + i\Omega_p^{*}\rho_{45}^{(1)}\big]/\Im_3, \tag{10c}$$

$$\rho_{23}^{(2)} = \big(-i\Omega_{23}\rho_{33}^{(2)} + i\Omega_{32}^{*}\rho_{22}^{(2)} - i\Omega_{21}^{*}\rho_{13}^{(2)} + i\Omega_{43}\rho_{24}^{(2)} + i\Omega_p^{*}\rho_{25}^{(1)}\big)/\Im_6, \tag{10d}$$

$$\rho_{21}^{(2)} = \big[-i\Omega_{32}\rho_{31}^{(2)} + i\Omega_{21}^{*}\big(\rho_{22}^{(2)} - \rho_{11}^{(2)}\big) + i\Omega_{41}^{*}e^{-i\phi}\rho_{24}^{(2)}\big]/\Im_5, \tag{10e}$$

$$\rho_{31}^{(2)} = \big(i\Omega_{32}^{*}\rho_{21}^{(2)} - i\Omega_{13}^{*}\rho_{41}^{(2)} + i\Omega_{41}^{*}e^{-i\phi}\rho_{34}^{(2)} + i\Omega_{21}^{*}\rho_{32}^{(2)} - i\Omega_p\rho_{51}^{(1)}\big)/\Im_8, \tag{10f}$$

$$\rho_{11}^{(2)} = \big(i\Omega_{41}e^{i\phi}\rho_{41}^{(2)} - i\Omega_{41}e^{i\phi}\rho_{14}^{(2)} - i\Omega_{21}^{*}\rho_{12}^{(2)}\big) + i\Omega_{21}\rho_{21}^{(2)}\big)/(2\gamma_{14} + 2\gamma_{12}), \tag{10g}$$

$$\rho_{22}^{(2)} = \big(2\gamma_{12}\rho_{11}^{(2)} + i\Omega_{32}\rho_{32}^{(2)} - i\Omega_{32}^{*}\rho_{23}^{(2)} + i\Omega_{21}^{*}\rho_{12}^{(2)} - i\Omega_{21}\rho_{21}^{(2)}\big)/2\gamma_{23}, \tag{10h}$$

$$\rho_{33}^{(2)} = \big(2\gamma_{43}\rho_{44}^{(2)} + 2\gamma_{23}\rho_{22}^{(2)} - i\Omega_{43}\rho_{34}^{(2)} + i\Omega_{43}^{*}\rho_{43}^{(2)} - i\Omega_{32}\rho_{32}^{(2)} + i\Omega_{32}^{*}\rho_{23}^{(2)} - i\Omega_p^{*}\rho_{35}^{(1)} + i\Omega_p\rho_{53}^{(1)}\big)/2\gamma_{35}, \tag{10i}$$

$$\rho_{44}^{(2)} = \big(2\gamma_{14}\rho_{11}^{(2)} + i\Omega_{43}\rho_{34}^{(2)} - i\Omega_{43}^{*}\rho_{43}^{(2)} + i\Omega_{44}^{*}\rho_{14}^{(2)} - i\Omega_{41}e^{i\phi}\rho_{41}^{(2)}\big)/2\gamma_{43}, \tag{10j}$$

where

$$\rho_{15}^{(1)} = -i\Omega_p(\Omega_{32}\Omega_{21}\Im_4 - \Omega_{43}\Omega_{41}e^{i\phi}\Im_7)/\Re, \tag{11a}$$

$$\rho_{25}^{(1)} = \Omega_p\big(-\Omega_{43}\Omega_{21}\Omega_{41}e^{i\phi} + \Omega_{32}\Omega_{41}^2 - \Omega_{32}\Im_4\Im_{10}\big)/\Re, \tag{11b}$$

$$\rho_{45}^{(1)} = \Omega_p\big(-\Omega_{32}\Omega_{21}\Omega_{41}e^{-i\phi} + \Omega_{43}\Omega_{21}^2 + \Omega_{43}\Im_7\Im_{10}\big)/\Re. \tag{11c}$$

The linear susceptibility $\chi^{(1)}$ and the third-order nonlinear susceptibility $\chi^{(3)}$ of the medium for the weak probe laser field are related to the atomic coherences as [1,37]

$$\chi^{(1)} = \frac{2N\wp_{53}^2}{\varepsilon_0\hbar\Omega_p}\rho_{35}^{(1)}, \tag{12}$$

$$\chi^{(3)} = \frac{2N\wp_{53}^4}{3\varepsilon_0\hbar\Omega_p^3}\rho_{35}^{(3)}, \tag{13}$$

where N is the atomic number density matrix and $\wp_{53}$ denotes the transition dipole moment between the levels $|3\rangle$ and $|5\rangle$. The analytical expression for first- and third-order susceptibilities depends on the controllable parameters of the system such as the detunings and intensities of the driving fields as well as the relative phase of applied fields. It is well known that the Kerr nonlinearity corresponds to the refraction part of the third-order susceptibility $\chi^{(3)}$, while the imaginary part of $\chi^{(3)}$ determines the nonlinear absorption [1]. The real and imaginary parts of $\chi^{(1)}$ correspond to the linear dispersion and absorption, respectively. The slope of the linear dispersion with respect to the probe detuning represents the group velocity of a weak probe field.

III. ENHANCED KERR NONLINEARITY

Now we focus on the third-order susceptibility behavior of the KR5 atomic system through numerical simulation. For linear and nonlinear susceptibilities we plot the curves in units of $\frac{2N\wp_{53}^2}{\varepsilon_0\hbar\Omega_p}$ and $\frac{2N\wp_{53}^4}{3\varepsilon_0\hbar^3\Omega_p^3}$, respectively. Here we are interested in the linear and nonlinear properties of the KR5 medium. The linear and nonlinear susceptibilities can be modified by the controlling parameters such as intensity and frequency detuning of coupling fields, i.e., Rabi frequencies, and relative phase between applied fields. Therefore, the giant Kerr nonlinearity with reduced linear and nonlinear absorption can be obtained under the condition of low light power.

The first- and third-order susceptibilities of a weak probe field are displayed in Fig. 2 for various values of the intensity of the applied fields. Here we assume that all of the coupling fields are in exact resonance with the corresponding transitions, so the multiphoton resonance condition is fulfilled, i.e., $\Delta = 0$. Figures 2(a) and 2(b) show that when $\phi = 0$ and $\Omega_{21} = \Omega_{32} = \Omega_{43} = \Omega_{41} = \gamma$, the first- and third-order susceptibility spectra have three linear and nonlinear absorption peaks. Figure 2(b) shows that the maximal Kerr nonlinearity is accompanied by large linear and nonlinear absorption around $\Delta_p = 0$. The slope of linear dispersion is negative at zero probe field detuning, which suggests superluminal light propagation. In this case, the group velocity is negative [Fig. 2(c)] and the medium is not suitable for application of low-intensity nonlinear optics due to the absorption losses. Figure 3 displays the curves for nonequal values of the coupling fields: $\Omega_{21} = 2\gamma$, $\Omega_{41} = 1.1\gamma$, $\Omega_{32} = \gamma$, and $\Omega_{43} = 1.9\gamma$. One can see that the central peaks of the linear and nonlinear absorption are split into four peaks in the absorption spectrum. Compared to Fig. 2, now the linear and nonlinear absorption reduce so that three reduced absorption windows appear around $\Delta_p = 0, \pm\delta$. Within these reduced absorption regions the slope of linear dispersion becomes positive. This represents the subluminal light propagation with the positive group velocity [Fig. 3(c)]. In addition, the increased Kerr nonlinearity appears inside reduced absorption windows. Thus, by properly adjusting the intensities of driving fields, one could achieve the enhanced Kerr nonlinearity accompanied by reduced absorption under the condition of slow light levels.

Figure 4 shows the transmission coefficient of the probe field propagating through the five-level atomic system. If all the Rabi frequencies are the same and equal to the decay

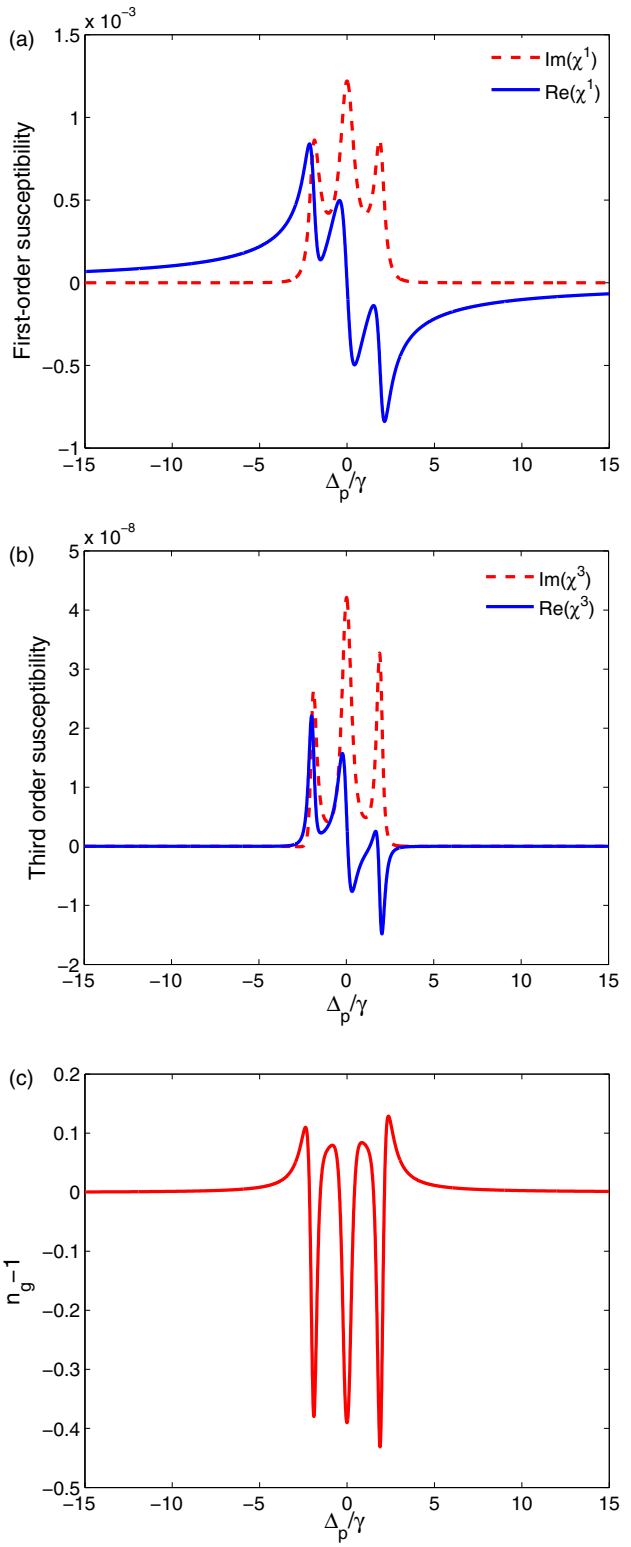

FIG. 2. (Color online) Linear and nonlinear susceptibility as well as group index versus probe field detuning. (a) Linear absorption (dashed line) and linear dispersion (solid line), (b) nonlinear absorption (dashed line) and Kerr nonlinearity (solid line), and (c) group index. The parameters are $\gamma_{14} = 0.8\gamma$, $\gamma_{12} = 0.1\gamma$, $\gamma_{23} = 0.1\gamma$, $\gamma_{43} = 0.4\gamma$, $\gamma_{35} = 0.02\gamma$, $\Omega_{21} = \Omega_{32} = \Omega_{43} = \Omega_{41} = \gamma$, $\Delta_{43} = \Delta_{23} = \Delta_{14} = \Delta_{12} = 0$, and $\phi = 0$. All the parameters are scaled with γ.

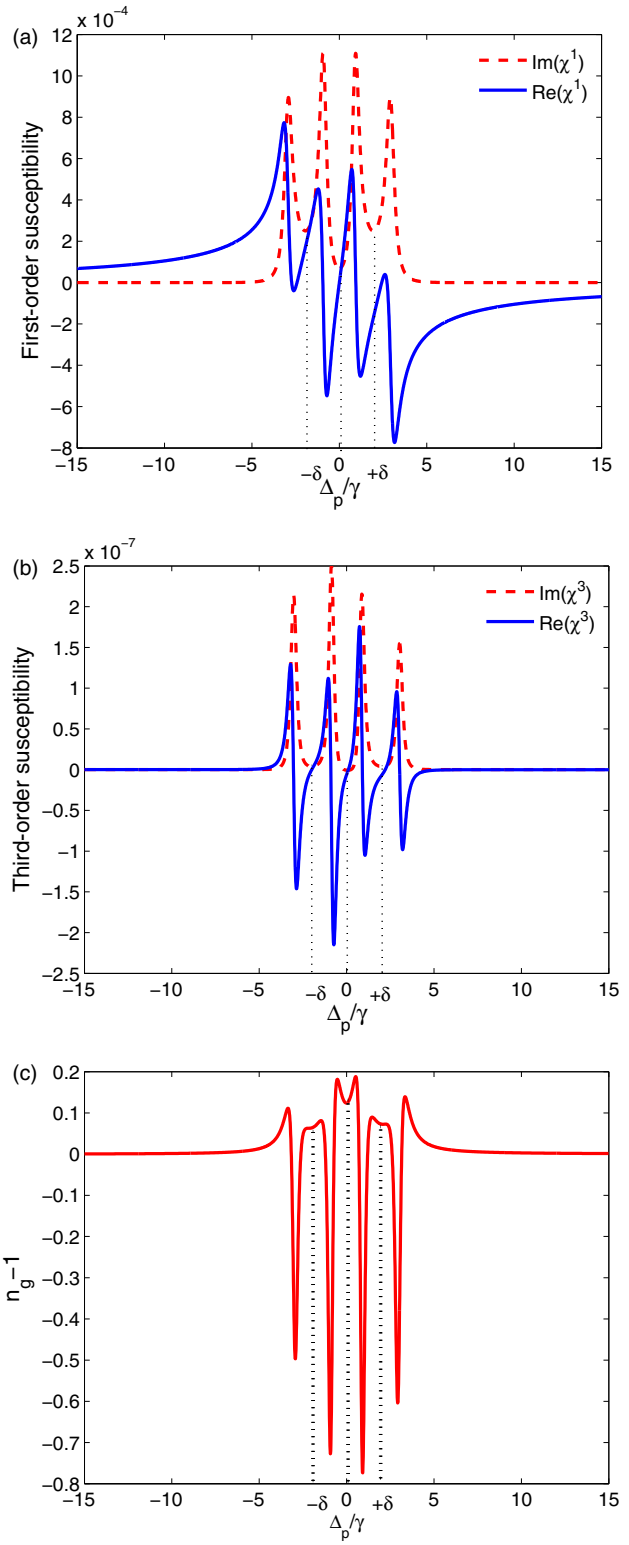

FIG. 3. (Color online) Linear and nonlinear susceptibility as well as group index versus probe field detuning. (a) Linear absorption (dashed line) and linear dispersion (solid line), (b) nonlinear absorption (dashed line) and Kerr nonlinearity (solid line), and (c) group index. The parameters are fields $\Omega_{21} = 2\gamma$, $\Omega_{41} = 1.1\gamma$, $\Omega_{32} = \gamma$, and $\Omega_{43} = 1.9\gamma$. The other parameters are the same as in Fig. 2.

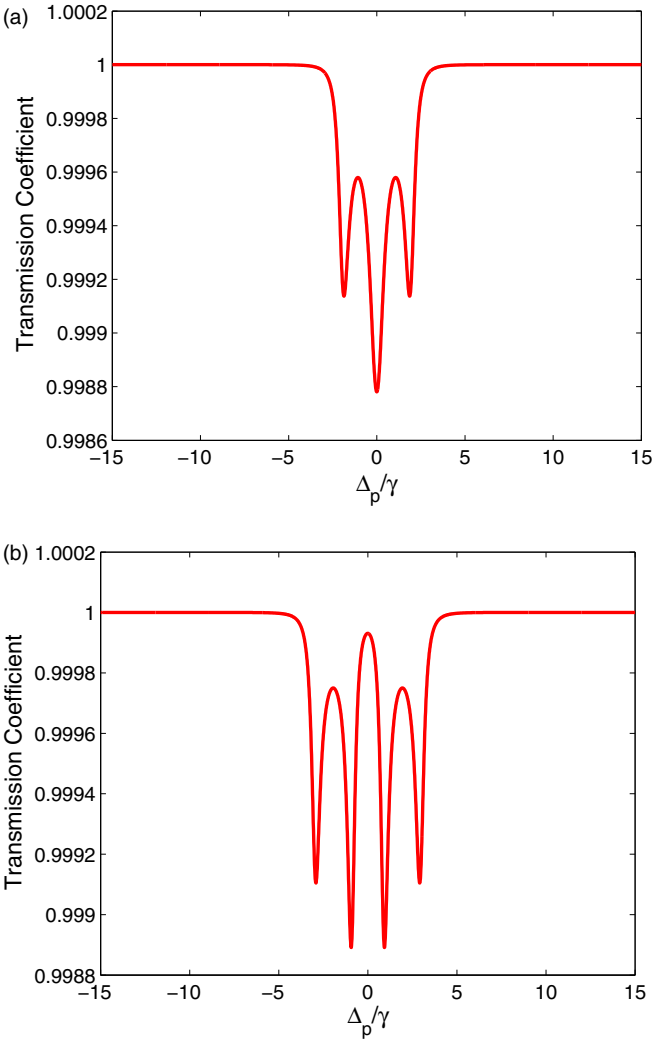

FIG. 4. (Color online) Transmission coefficient versus probe field detuning for (a) $\Omega_{21} = \Omega_{32} = \Omega_{43} = \Omega_{41} = \gamma$ and (b) $\Omega_{21} = 2\gamma$, $\Omega_{41} = 1.1\gamma$, $\Omega_{32} = \gamma$, and $\Omega_{43} = 1.9\gamma$. The other parameters are the same as in Fig. 2.

rate $\Omega_{21} = \Omega_{32} = \Omega_{43} = \Omega_{41} = \gamma$, the medium has a low transmission in the vicinity of the zero probe detuning and there are another two transmission dips for nonzero detuning, as one can see in Fig. 4(a). For nonequal Rabi frequencies $\Omega_{21} = 2\gamma$, $\Omega_{41} = 1.1\gamma$, $\Omega_{32} = \gamma$, and $\Omega_{43} = 1.9\gamma$, the number of transmission dips converts to 4 [see Fig. 4(b)]. Moreover, the transmission coefficient approaches unity at zero detuning $\Delta_p = 0$. These results are in agreement with the probe absorption spectra given in Figs. 2 and 3.

A comparison is also made in Fig. 5 between the Kerr-nonlinear coefficients of the five-level KR5 system with that of the existing four- and three-level cascade-type atomic systems. Note that in the four-level system, level $|2\rangle$ is neglected ($\Omega_{21} = \Omega_{32} = 0$) [see Fig. 1(b)], while for the three-level cascade-type system, both atomic levels $|2\rangle$ and $|1\rangle$ are neglected ($\Omega_{21} = \Omega_{32} = \Omega_{41} = 0$) [see Fig. 1(c)]. It is realized that the magnitude of Kerr nonlinearity for the five-level KR5 system is larger than that of four- and three-level systems. This indicates an advantage of employing such a scheme in enhancing the Kerr nonlinearity rather than its

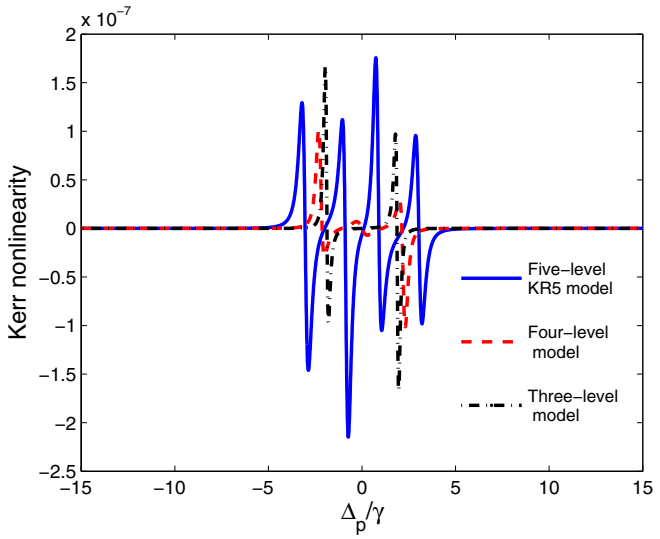

FIG. 5. (Color online) Kerr-nonlinear indices in the case of the five-level KR5 system (solid line), the four-level cascade system (dashed line), and the three-level cascade system (dotted line). The parameters are the same as in Fig. 3, except those for the four-level case where $\Omega_{21} = \Omega_{32} = 0$, whereas for the three-level case one has $\Omega_{21} = \Omega_{32} = \Omega_{41} = 0$.

existing three- and four-level atomic counterparts. Moreover, as mentioned earlier, another type of five-level atomic system has recently been examined for exploring the Kerr-nonlinearity enhancement [26]. In this type of five-level configuration, a weak probe field drives the lower transition, while an intense coupling beam couples simultaneous transitions between the intermediate level and three upper closely spacing states. Then the magnitude of Kerr nonlinearity for such a five-level cascade-type scheme is compared with that of the four- and three-level cascade-type systems. Although compared to the existing four- and three-level schemes this type of five-level configuration can exhibit a wider spectral region of enhanced Kerr nonlinearity with more positive and negative peaks, its maximal Kerr nonlinearity is the same as that of the existing three- and four-level cascade systems.

In fact, both types of five-level KR5 system proposed here and the cascade-type system proposed in Ref. [26] are based on the ladder-type three-level system in which the upper transition is driven by a strong field. However, in Ref. [26] the single upper transition in the ladder-type system is replaced by simultaneous transitions between an intermediate level and three upper closely spacing states. In our proposal, the single upper transition is replaced by multiple transitions driven by four laser fields that form a diamond-shape closed-loop structure. We found that by increasing the number of levels in such a way that they form a consequently coupled cyclic chain of four states coupled to the ground state [Figs. 1(a)–1(c)], it is possible to realize higher orders of nonlinearity, while the same magnitude of Kerr nonlinearity among the three systems was observed in Ref. [26]. This shows an advantage of employing such a five-level system in producing higher Kerr nonlinearity over that considered in Ref. [26].

Consider next the effect of coupling field detunings on the Kerr nonlinearity. Figure 6 shows the real (dispersion) and imaginary (absorption) parts of linear and nonlinear susceptibilities versus the relative phase between applied fields. Illustrated in Figs. 6(a) and 6(b) is a situation where the applied fields are in an exact resonance with the corresponding transitions, i.e., $\Delta_{43} = \Delta_{23} = \Delta_{14} = \Delta_{12} = 0$. One can see that the Kerr nonlinearity is accompanied by large linear and nonlinear absorption. Furthermore, the linear dispersion is negative, which corresponds to the superluminal light propagation. Using the supposition that the fields Ω_{43} and Ω_{32} are not in resonance with the corresponding atomic transitions ($\Delta_{43} = \Delta_{23} = 2\gamma$), we plot the first- and third-order susceptibility spectra versus ϕ in Figs. 6(c) and 6(d). Note that the multiphoton resonance condition $\Delta = 0$ is still kept. One can see that the giant Kerr nonlinearity is accompanied by the reduced linear and nonlinear absorption for all relative phases ϕ. Also, the linear dispersion is now positive providing the slow light.

IV. PHASE CONTROL OF KERR NONLINEARITY

Expressions (7)–(11) and Fig. 6 show that the linear and nonlinear susceptibilities can be controlled by the relative phase of the applied fields. Now we provide an analytical model to understand such phase control. Four driving fields Ω_{43}, Ω_{32}, Ω_{21}, and Ω_{41} acting on the atom build a closed-loop level scheme in which the relative phase ϕ between applied fields affects linear and nonlinear optical properties of the medium. Excluding in Eq. (1) the ground (or metastable) state $|5\rangle$, the Hamiltonian of the atom-light interaction for the remaining atomic four-level closed-loop level scheme of diamond shape can be rewritten as

$$H_{\text{4-level}} = -\hbar\Omega \left[|1\rangle\, e^{i\phi}\, \langle 4| + \sum_{j=1}^{3} |j+1\rangle\, \langle j| + \text{H.c.} \right]. \tag{14}$$

In addition, the amplitudes of all Rabi frequencies in Eq. (14) are chosen to be the same, i.e.,

$$\Omega_{43} = \Omega_{32} = \Omega_{41} = \Omega_{21} = \Omega. \tag{15}$$

The Hamiltonian (14) is equivalent to its counterpart involving an infinite number of states

$$H_0 = -\hbar\Omega \sum_{j=-\infty}^{\infty} |j+1\rangle\, \langle j| + \text{H.c.} \tag{16}$$

as long as the coefficients c_j entering any state vector $|\cdots\rangle = \sum_j c_j |j\rangle$ obey the boundary conditions

$$c_{j+4} = e^{i\phi} c_j\,. \tag{17}$$

For $\phi = 0$, Eq. (17) reduces to the usual periodic boundary conditions. On the other hand, for $\phi = \pm\pi$, Eq. (17) represents the twisted boundary conditions.

The Hamiltonian given by Eqs. (14)–(17) can be easily diagonalized [38] and its eigenstates and corresponding eigenenergies read

$$|n(r)\rangle = \frac{1}{2} \sum_{j=1}^{4} |j\rangle e^{i q_n j}, \quad E_n = -2\hbar\Omega \cos q_n, \tag{18}$$

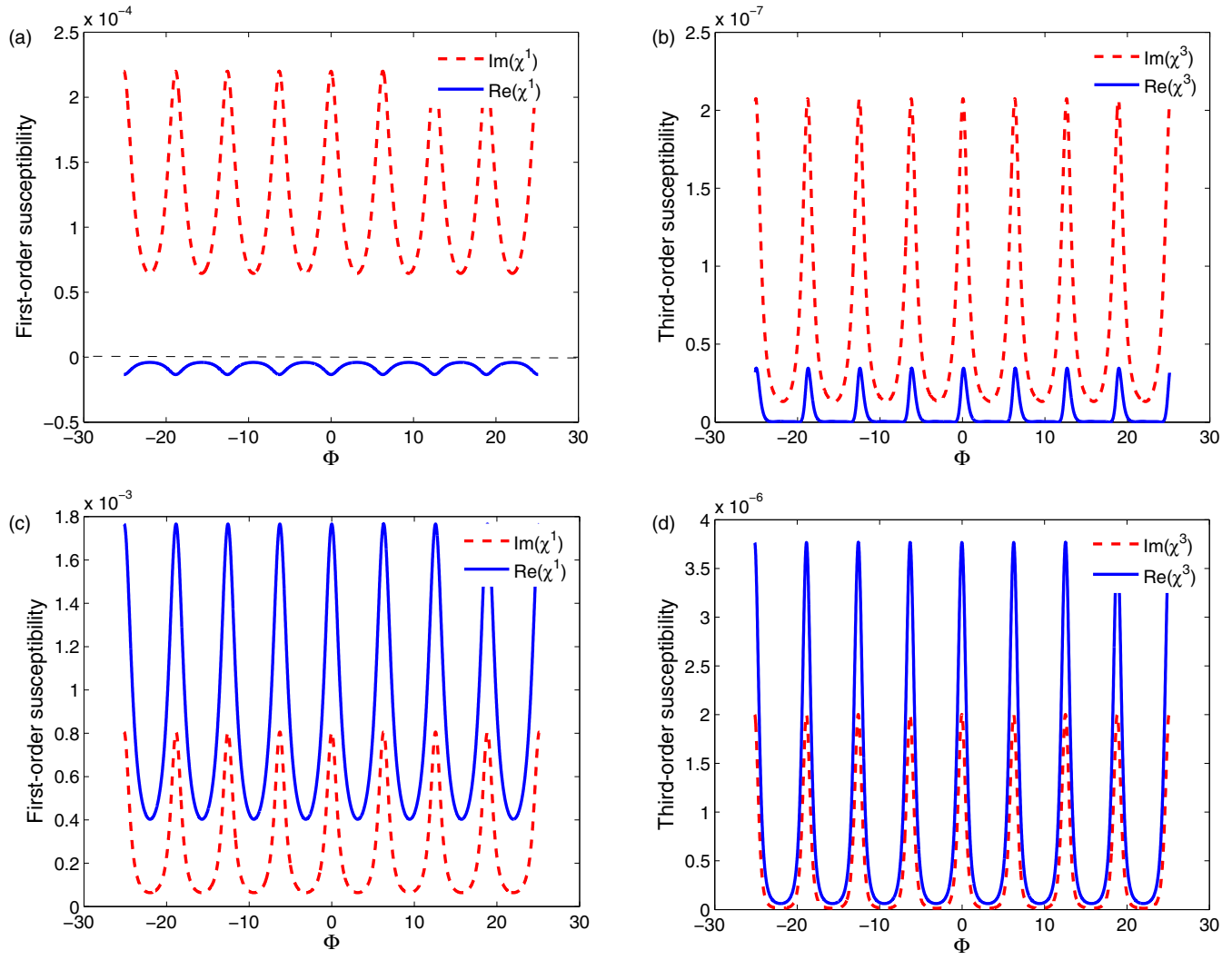

FIG. 6. (Color online) (a) and (c) Linear and (b) and (d) nonlinear susceptibility versus relative phase ϕ for (a) $\Delta_{43} = \Delta_{23} = \Delta_{14} = \Delta_{12} = 0$ and (b) $\Delta_{43} = \Delta_{23} = 2\gamma$ and $\Delta_{14} = \Delta_{12} = 0$. The parameters are $\Omega_{21} = 5\gamma$, $\Omega_{41} = 3\gamma$, $\Omega_{32} = \gamma$, and $\Omega_{43} = 2\gamma$. The other parameters are the same as in Fig. 2.

where n=1,2,3,4. The dimensionless parameter q_n takes a set of values that depends on the relative phase ϕ,

$$q_n = \frac{(n-1)\pi}{2} - \frac{\phi}{4}, \quad n = 1,2,3,4. \tag{19}$$

Let we now analyze the eigenenergies for different phase ϕ by taking $\Omega = 2\gamma$. For condition (i) $\phi = 0$ ($\Omega_{43} = \Omega_{32} = \Omega_{41} = \Omega_{21} = \Omega$), Eq. (18) becomes $E_n = -2\hbar\Omega \sin(\frac{n\pi}{2})$, so the eigenenergies are

$$E_3 = -E_1 = 2\hbar\Omega, \quad E_2 = E_4 = 0. \tag{20}$$

Three different eigenenergies shown in Fig. 1(d) can be attributed to three peaks in the absorption profile in Figs. 7(a) and 7(b). In this case, the interacting dark resonances will be established.

For condition (ii) $\phi = \frac{\pi}{2}$ ($\Omega_{43} = \Omega_{32} = \Omega_{41} = \Omega_{21} = \Omega$) we have $E_n = -2\hbar\Omega \sin(\frac{n\pi}{2} - \frac{\pi}{8})$, providing the following eigenenergies:

$$\begin{aligned} E_3 &= -E_1 = 4\hbar\gamma \cos\frac{\pi}{8}, \\ E_4 &= -E_2 = 4\hbar\gamma \sin\frac{\pi}{8}. \end{aligned} \tag{21}$$

Now four different eigenenergies are obtained. Thus, four absorption peaks appear for $\phi = \pi/2$, as one can see in Figs. 1(e), 7(c), and 7(d). In other words, the central peaks of linear and nonlinear absorption profiles split and for $\phi = \pi/2$ we have four absorption peaks.

For condition (iii) $\phi = \pi$ ($\Omega_{43} = \Omega_{32} = \Omega_{41} = \Omega_{21} = \Omega$) we have $E_n = -2\hbar\Omega \sin(\frac{n\pi}{2} - \frac{\pi}{4})$, giving the eigenenergies

$$E_1 = E_2 = -\sqrt{2}\hbar\Omega, \quad E_3 = E_4 = \sqrt{2}\hbar\Omega. \tag{22}$$

It is easy to see that there is a twice degenerate ground level (containing the states with $n = 1$and 2) and a twice degenerate excited level ($n = 3$ and 4) separated by the energy $|\sqrt{2}\hbar\Omega|$, as shown in Fig. 1(f). Therefore, two different eigenenergies are obtained, yielding two peaks in the absorption profile in

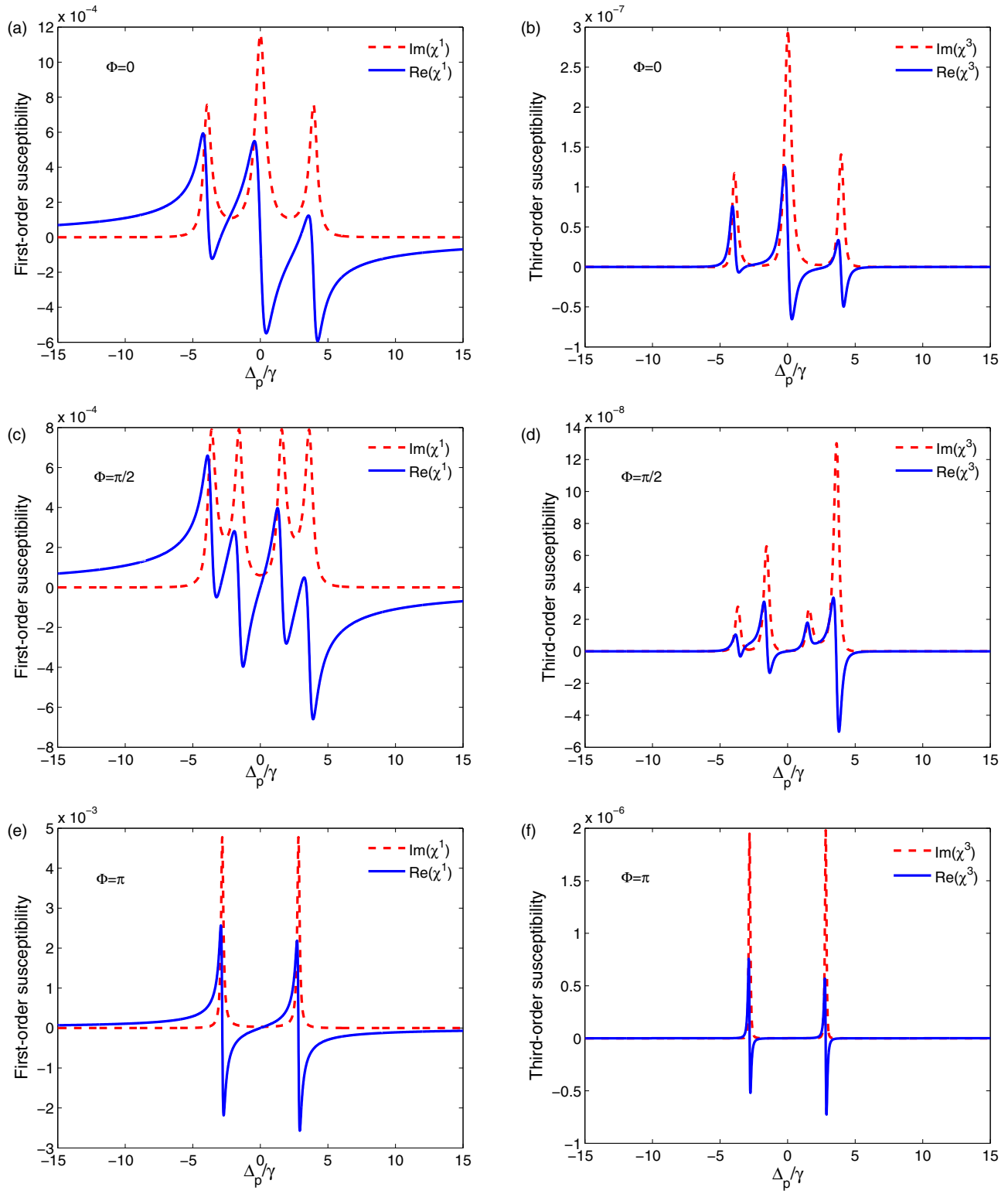

FIG. 7. (Color online) Phase control of (a), (c), and (e) linear and (b), (d), and (f) nonlinear susceptibility for (a) and (b) $\phi = 0$, (c) and (d) $\phi = \pi/2$, and (e) and (f) $\phi = \pi$. Here $\Omega_{21} = \Omega_{32} = \Omega_{43} = \Omega_{41} = 2\gamma$ and the other parameters are the same as in Fig. 2.

Figs. 7(e) and 7(f). Consequently, the double-dark-resonance structure is not established for $\phi = \pi$ and just two side peaks are formed in the absorption spectrum.

A three-dimensional plot of the steady-state linear and nonlinear absorption spectra versus Δ_p and ϕ can provide a better perspective of this phenomenon, as shown in Fig. 8. One can see that by changing the relative phase ϕ, the medium can have three, four, and two absorption peaks. It should be noted that in Fig. 7 the Kerr nonlinearity experiences a large nonlinear absorption. Therefore, we find a wide range of

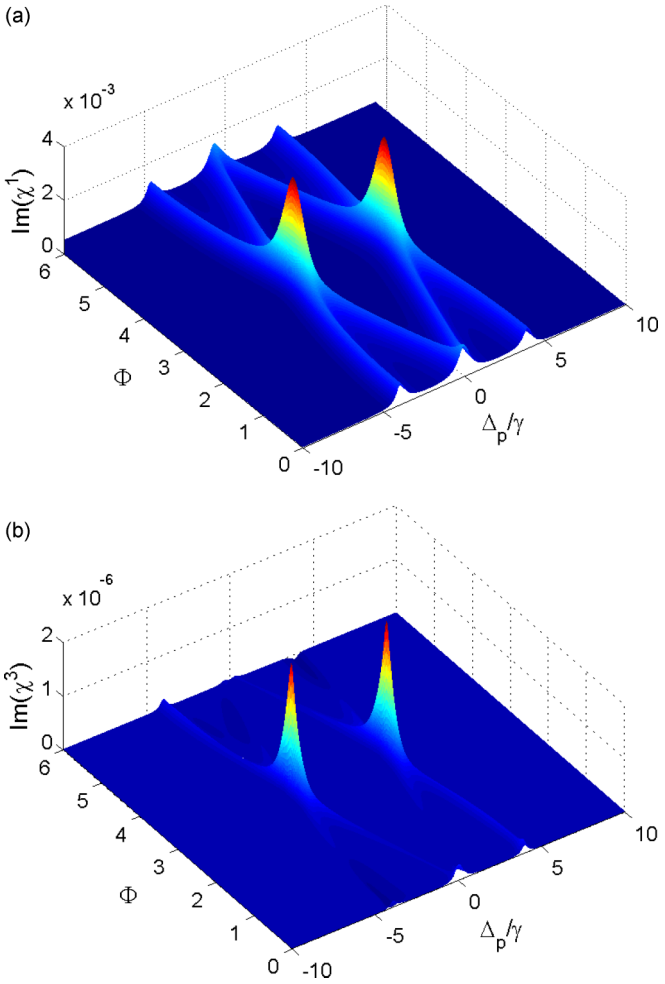

FIG. 8. (Color online) Three-dimensional plot of phase control of (a) linear and (b) nonlinear susceptibility Here the parameters are the same as in Fig. 6.

tunability in the linear and nonlinear absorption and dispersion just by adjusting the relative phase of the applied fields.

Using the above analytical model, now we can explain the physical mechanism of the Kerr-nonlinearity enhancement obtained in Figs. 2 and 3. Figure 2 is plotted for the parameters satisfying condition (i) ($\Omega_{21} = \Omega_{32} = \Omega_{43} = \Omega_{41} = \gamma$ and $\phi = 0$). Therefore, three absorption peaks observed in Fig. 2 reflect the eigenenergies given in Eq. (20). The central peaks in both the linear and nonlinear absorption profiles separate two reduced absorption windows and show a double-dark-resonance structure, whereas two absorption peaks located on both sides of the central frequency detuning $\Delta_p = 0$ represent one photon transition [35]. In fact, in such a scheme there is coherent population trapping (CPT), which may lead to reduced absorption windows on the left- and right-hand sides of $\Delta_p = 0$. Since an ideal CPT medium does not interact with the light, it also cannot produce any nonlinear effects [37]. When we change the coupling fields to $\Omega_{21} = 2\gamma$, $\Omega_{41} = 1.1\gamma$, $\Omega_{32} = \gamma$, and $\Omega_{43} = 1.9\gamma$ (see the parameter condition used in the plot of Fig. 3), the Rabi frequencies of the applied fields exceed those in condition (i). Thus the CPT is disturbed, leading to a strong nonlinear coupling between the electromagnetic fields interacting with the atomic system. In this case, the eigenenergies for the Hamiltonian (14) read [35]

$$E_1 = -\frac{(y+m^{1/2})^{/2}}{2^{/2}}, \quad E_2 = -\frac{(y-m^{1/2})^{/2}}{2^{/2}}, \\ E_3 = \frac{(y-m^{1/2})^{/2}}{2^{/2}}, \quad E_4 = \frac{(y-m^{1/2})^{/2}}{2^{/2}}, \tag{23}$$

with

$$\begin{aligned} k &= \Omega_{43}^2 - \Omega_{32}^2 + \Omega_{41}^2 - \Omega_{21}^2, \\ l &= \Omega_{43}^2 + \Omega_{32}^2 + \Omega_{41}^2 + \Omega_{21}^2, \\ m &= l^2 - 4(\Omega_{41}\Omega_{32} - \Omega_{43}\Omega_{21})^2, \\ n &= \Omega_{41}\left(\Omega_{43}^2 - \Omega_{32}^2 + \Omega_{21}^2\right) + \Omega_{41}^3 + 2\Omega_{43}\Omega_{21}\Omega_{32}, \\ s &= \Omega_{43}\left(\Omega_{41}^2 - \Omega_{21}^2 + \Omega_{32}^2\right) + \Omega_{43}^3 + 2\Omega_{41}\Omega_{21}\Omega_{32}, \\ w &= \Omega_{43}\Omega_{32} + \Omega_{41}\Omega_{21}. \end{aligned} \tag{24}$$

Evidently, the four eigenenergies given in Eq. (23) correspond to four absorption peaks in linear and nonlinear susceptibilities. This condition was demonstrated in Fig. 3.

V. TIME-DEPENDENT KERR NONLINEARITY

In the following we discuss the temporal evolution of the Kerr nonlinearity in the KR5 atomic system and investigate the optical switching time in the nonlinear regime by using the numerical result from the density-matrix equations of motion.

Figure 9 illustrates the transient behavior of the probe linear absorption and dispersion for various values of the detuning parameters Δ_{43} and Δ_{23}. The selected parameters are the same as in Fig. 5, unless $\Delta_p = 0.1\gamma$ and $\phi = \pi$. Figure 9 shows an optical switching process in which a weak Kerr index with superluminal absorption switches to the EIT-based slow light giant Kerr nonlinearity by changing $\Delta_{43} = \Delta_{23}$ from 0 to γ. According to Figs. 9(a) and 9(b), after a short oscillatory behavior, the linear absorption and dispersion curves reach the steady-state limit. However, when the laser beams described by the Rabi frequencies Ω_{43} and Ω_{32} are in resonance ($\Delta_{43} = \Delta_{23} = 0$), the steady-state value of the linear absorption coefficient is positive, while the steady-state value of the linear dispersion is negative. This condition suggests a superluminal absorption. Similar curves are plotted for the case of nonresonant detuning ($\Delta_{43} = \Delta_{23} = \gamma$). With an increase of time, the steady-state value of the linear absorption is reduced and finally the EIT appears. Furthermore, the steady-state linear dispersion changes its sign to a positive value corresponding to the subluminal light propagation.

A temporal behavior of the Kerr nonlinearity is also displayed in Fig. 9(c). It can be seen that the curves for the Kerr-nonlinear coefficient exhibit a transient oscillatory behavior for a short time and then reach a steady-state value. Also, for $\Delta_{43} = \Delta_{23} = \gamma$ the steady-state Kerr nonlinearity is gradually enhanced compared to the case $\Delta_{43} = \Delta_{23} = 0$. Therefore, by going out of resonance, the enhanced Kerr nonlinearity accompanied by subluminal assistant EIT is obtained.

Let us now analyze the phase-sensitive switching feature of the Kerr nonlinearity in the pulsed regime for the KR5 atomic

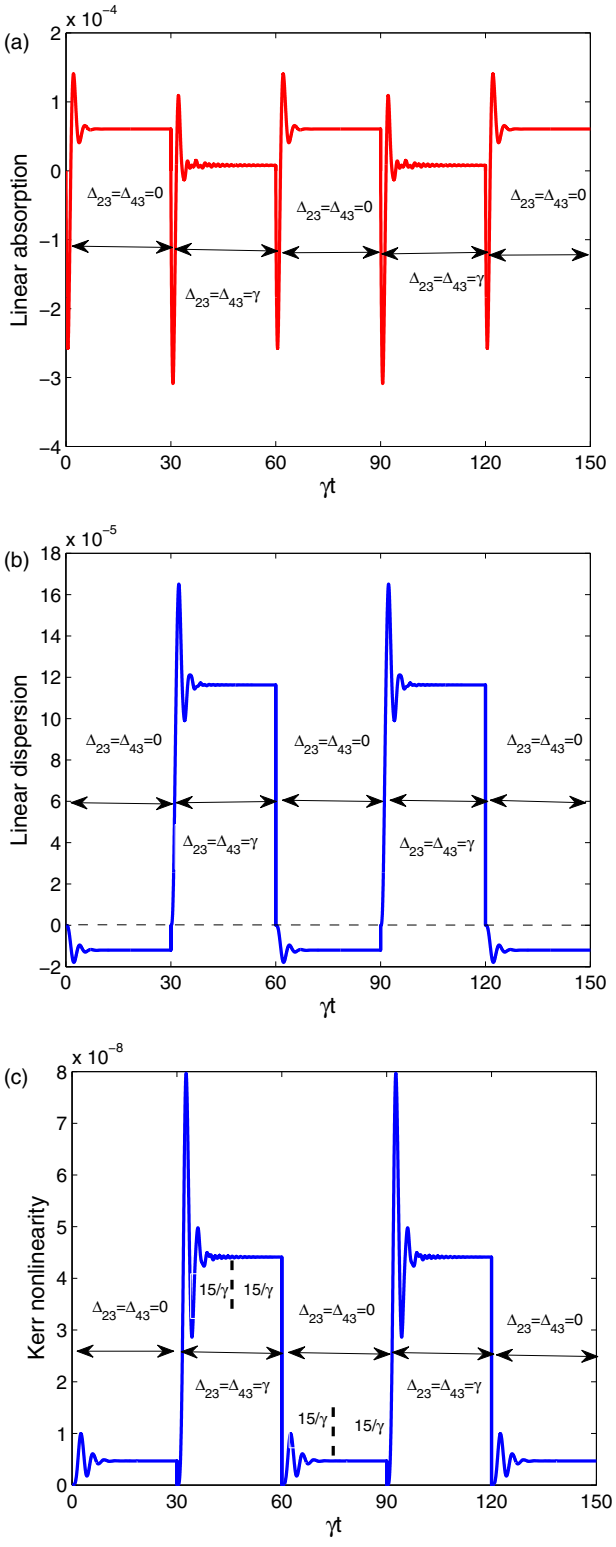

FIG. 9. (Color online) Switching process of the (a) linear absorption, (b) linear dispersion, and (c) Kerr nonlinearity for different values of Δ_{43} and Δ_{23}. Here $\Delta_p = 0.1\gamma$, $\phi = \pi$, and the other parameters are the same as in Fig. 5.

system. Figure 10 shows that the oscillation frequency of the Kerr nonlinearity increases as the relative phase changes from $\phi = \pi$ to $\phi = \pi/2$. In a similar manner, the magnitude of the steady-state value of the Kerr nonlinearity can be increased.

We now demonstrate that this system can be used as an optical switch for nonlinear dispersion in which a weak Kerr nonlinearity can be converted to a giant one. It can be seen from Figs. 8(c) and 9 that the switching time needed to convert a weak nonlinear dispersion into an enhanced one and vice versa equals approximately $15/\gamma$. Considering the D_1 line of the ^{87}Rb atom with the typical decay rate $\gamma \simeq 36$ MHz, we can obtain a nonlinear switching time equal to approximately 416 nm.

Thus, we demonstrated that this KR5 medium can be employed as an optical switch in which the propagation of the laser pulse can be controlled by another laser field that is useful for an optically controlled optical device. The results presented may be useful for understanding the switching feature of the EIT-based slow light Kerr nonlinearity, have potential application in optical information processing and transmission, and may be helpful for the realization of fast optical nonlinearities and optically controlled optical devices. A high-speed optical switch is an important technique for quantum information networks [39,40].

VI. DOPPLER BROADENING AND KERR NONLINEARITY

At room or higher temperatures there is a broad distribution of atomic velocities. Thus, the Doppler shift cannot be neglected and must be taken into account [41,42]. The effect of the Doppler broadening due to the atom's thermal velocity υ can be included by replacing Δ_{12}, Δ_{14}, Δ_{23}, and Δ_{43} by $\Delta_{12} - k\upsilon$, $\Delta_{14} - k\upsilon$, $\Delta_{23} - k\upsilon$, and $\Delta_{43} - k\upsilon$, respectively. Here all the laser fields are assumed to copropagate in the same direction $k_1 \simeq k_2 \simeq k_3 \simeq k_4 \simeq k_p = k$, where k_p,k_i ($i = 1,2,3,4$) are the wave vectors of the probe and driving fields, respectively.

Using the Maxwell velocity distribution, we obtain

$$\Upsilon(\upsilon) = (2\pi)^{-1/2} w^{-1} e^{-\upsilon^2/w^2}, \tag{25}$$

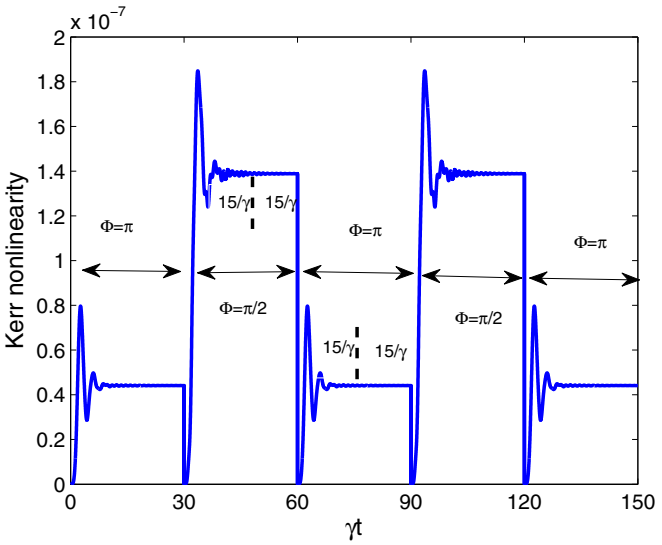

FIG. 10. (Color online) Switching process of the Kerr nonlinearity for different values of ϕ. Here $\Delta_{43} = \Delta_{23} = \gamma$ and the other parameters are the same as in Fig. 5.

where $w = (\frac{2k_BT}{m})^{1/2}$ is the Doppler width. Relating the probe susceptibility χ to the coherence term ρ_{35} and utilizing Eq. (4), the linear and nonlinear susceptibilities of the probe field then read

$$\chi^{(1)}(\Delta_p) = \int_{-\infty}^{\infty} \Upsilon(\upsilon)\chi^{(1)}(\Delta_p,\upsilon)d\upsilon, \tag{26a}$$

$$\chi^{(3)}(\Delta_p) = \int_{-\infty}^{\infty} \Upsilon(\upsilon)\chi^{(3)}(\Delta_p,\upsilon)d\upsilon, \tag{26b}$$

which gives the first- and third-order susceptibilities in the Doppler-broadened atomic system. Now we can analyze the behavior of the absorption and dispersion as well as the Kerr-nonlinear coefficient inside the Doppler-broadened medium. Figure 11 shows the effect of Doppler broadening on the linear and nonlinear susceptibilities. The chosen parameters are the same as those we used to plot Fig. 2.

In Figs. 11(a) and 11(b) we chose the Doppler width below the natural linewidth of the probe transitionγ ($kw = 0.1\gamma$). Obviously, the linear susceptibility is very similar in shape to the case without the Doppler broadening [see Fig. 2(a)], while a considerable change in shape is observed in the nonlinear susceptibility so that the slope of Kerr nonlinearity becomes positive around $\Delta_p = 0$. This indicates that, compared to the linear response of the KR5 system, the nonlinear response of the medium is more sensitive to the Doppler-broadening effect. Moreover, although the Kerr nonlinearity in Fig. 11(b) still experiences strong linear and nonlinear absorption, the Kerr-nonlinearity index is greatly enhanced compared to the nonbroadened case shown in Fig. 2. This result is completely different from the Kerr-nonlinearity enhancement due to EIT, which was presented earlier in this paper and in most of the relevant studies (see, for instance, [19,21,23–26]). Thus, we could achieve a large nonlinear Kerr coefficient for the probe field while maintaining linear and nonlinear absorption. The main advantage of this method over the EIT is that in the present method there is no need to adjust the laser fields to the strong intensities. However, the disadvantage is that the linear and the nonlinear absorption do not cancel. It should be noted that in order to obtain a Doppler-free arrangement in the room temperature cell, one can adjust the laser direction. However, the best way to eliminate the effect of Doppler broadening is to employ a cold-atom sample.

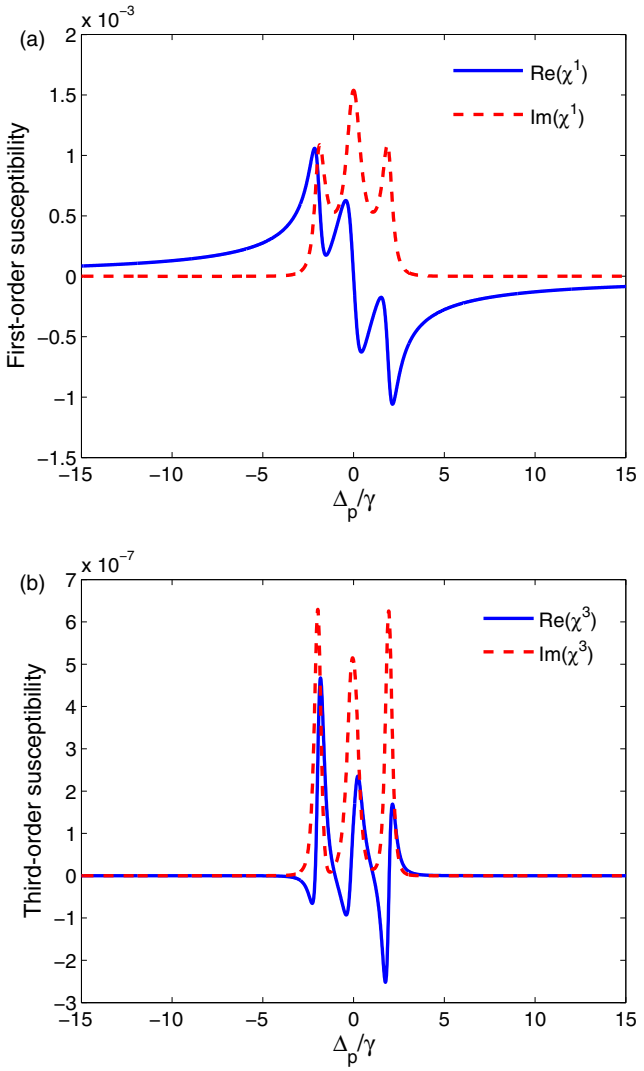

FIG. 11. (Color online) (a) Linear and (b) nonlinear susceptibility probe field detuning Δ_p including the Doppler broadening $kw = 0.1\gamma$. The parameters are the same as in Fig. 2.

VII. PRACTICAL OBSERVATION OF THE FIVE-LEVEL SCHEME

A possible experimental realization of the proposed scheme for the five-level KR5 structure can be implemented for the ^{87}Rb atomic system. The ground level $|5\rangle$ can be assigned to the $5S_{1/2}$ state. The level $|3\rangle$ can be attributed to the $5P_{3/2}$ state. Two intermediate levels $|2\rangle$ and $|4\rangle$ can be assigned to either the fine structure of the $4D_{3/2}$ substate or the $4D_{5/2}$ substate, as long as the dipole transition selection rules on the F quantum number are satisfied (the same F quantum number for the intermediate states). The top level $|1\rangle$ can be assigned to the $6P_{3/2}$ state.

Another physically realistic model is the scheme suggested with Kobrak and Rice to extend the theory of the stimulated Raman adiabatic passage [32]. One can consider the case of two-photon dissociation of the sodium dimer Na_2, which was examined experimentally by Shapiro *et al.* [43]. Here $|5\rangle$ is chosen to be the $\upsilon = 0, J = 33$ level of the sodium dimer ground state $^1\Sigma_g$ to simulate a component of the thermal population in a heat pipe [43]. The pump laser couples the ground state to the level $|3\rangle$ that is formed by spin-orbit coupling [44] the $\upsilon = 32, J = 32$ level of $A\,^1\Sigma_u$ with the $\upsilon = 33, J = 32$ level of the triplet state $b\,^3\Pi_u$.

In practice, as shown by Xia *et al.* [45], the triplet and singlet g-parity Rydberg states in a sodium dimer can be mixed by the spin-orbit interaction to form a series of coupled pairs. The triplet state is then excited to the continuum via the Stokes pulse and from there coupled to the branch state $b\,^3\Pi_u$ ($\upsilon = 93, J = 32$) [see Fig. 1(a)]. In the original calculation made by Shapiro *et al.*, three triplet electronic states were included in the continuum, corresponding to the photodissociation reactions $Na_2 \rightarrow Na(3p) + Na(3s)$, $Na_2 \rightarrow Na(4s) + Na(3s)$, and $Na_2 \rightarrow Na(3d) + Na(3s)$. However, they mentioned that the production of $Na(4s)$ is negligible in all cases.

VIII. CONCLUSION

The Kerr-nonlinearity behavior of a five-level quantum system has been investigated theoretically. It is shown that an enormous Kerr coefficient with reduced absorption can be obtained under the condition of the subluminal light propagation just by properly tuning of the applied fields. When the multiphoton resonance condition is established, one can achieve large subluminal Kerr nonlinearities with a negligible absorption in a wide range of relative phases by adjusting the detuning parameters. It is shown that the nonlinear dispersion and absorption of our system involving the closed-loop atomic transitions are strongly susceptible to the relative phase of the applied fields. An analytical model is presented to elucidate such phase control of the Kerr nonlinearity. We made a comparison between the nonlinear Kerr coefficients for the five-level KR5 scheme with that of the existing three- and four-level cascade-type systems. We found that the magnitude of Kerr nonlinearity is larger than that of the three- and four-level counterparts. This means that increasing the number of levels can lead the higher orders of nonlinearity. Finally, the influence of the Doppler broadening on linear and nonlinear susceptibilities was discussed.

ACKNOWLEDGMENT

This work was supported by the Lithuanian Research Council (Grant No. VP1-3.1-ŠMM-01-V-03-001).

[1] R. W. Boyd, *Nonlinear Optics* (Academic, San Diego, 1992).
[2] Y. Wu and L Deng, Opt. Lett. **29**, 2064 (2004).
[3] M. M. Kash, V. A. Sautenkov, A. S. Zibrov, L. Hollberg, G. R. Welch, M. D. Lukin, Y. Rostovtsev, F. S. Fry, and M. O. Scully, Phys. Rev. Lett. **82**, 5229 (1999).
[4] A. Imamouglu, H. Schmidt, G. Woods, and M. Deutsch, Phys. Rev. Lett. **79**, 1467 (1997).
[5] Y. Wu and X Yang, Phys. Rev. A **71**, 053806 (2005).
[6] S. E. Harris, Phys. Today **50** (7), 36 (1997).
[7] S. E. Harris, J. E. Field, and A. Imamoğlu, Phys. Rev. Lett. **64**, 1107 (1990).
[8] Y. Zhang, B. Anderson, and M. Xiao, Phys. Rev. A **77**, 061801 (2008); Y. Zhang, U. Khadka, B. Anderson, and M. Xiao, Phys. Rev. Lett. **102**, 013601 (2009).
[9] Y. Wu, J. Saldana, and Y. Zhu, Phys. Rev. A **67**, 013811 (2003); Y. Wu and X. Yang, *ibid.* **70**, 053818 (2004).
[10] C. Ding, R. Yu, J. Li, X. Hao, and Y. Wu, Phys. Rev. A **90**, 043819 (2014).
[11] J.-H. Li, X.-Y. Lü, J.-M. Luo, and Q.-J. Huang, Phys. Rev. A **74**, 035801 (2006); J.-H. Li, Phys. Rev. B **75**, 155329 (2007).
[12] Z. Wang, A.-X. Chen, Y. Bai, W.-X. Yang, and R.-K. Lee, J. Opt. Soc. Am. B **29**, 2891 (2012).
[13] Y. Wu and L. Deng, Phys. Rev. Lett. **93**, 143904 (2004).
[14] G. Huang, L. Deng, and M. G. Payne, Phys. Rev. E **72**, 016617 (2005).
[15] W.-X. Yang, J.-M. Hou, and R.-K. Lee, Phys. Rev. A **77**, 033838 (2008).
[16] L.-G. Si, W.-X. Yang, X.-Y. Lü, X. Hao, and X. Yang, Phys. Rev. A **82**, 013836 (2010).
[17] L. Li and G. Huang, Phys. Rev. A **82**, 023809 (2010).
[18] C. Hang and G. Huang, Opt. Express **18**, 2952 (2010); C. Zhu and G. Huang, *ibid.* **19**, 23364 (2011).
[19] H. Wang, D. Goorskey, and M. Xiao, Opt Lett. **27**, 258 (2002).
[20] Y. Niu and S. Gong, Phys. Rev. A **73**, 053811 (2006).
[21] Y. Niu, S. Gong, R. Li, Z. Xu, and X. Liang, Opt Lett. **30**, 3371 (2005).
[22] W.-j. Jiang, X. Yan, J.-p. Song, H.-b. Zheng, C. Wu, B.-y. Yin, and Y. Zhang, Opt. Commun. **282**, 101 (2009).
[23] S. H. Asadpour, H. R. Hamedi, and M. Sahrai, J. Lumin. **132**, 2188 (2012).
[24] Y. Han, J. Xiao, Y. Liu, C. Zhang, H. Wang, M. Xiao, and K. Peng, Phys. Rev. A **77**, 023824 (2008).
[25] J. Sheng, X. Yang, H. Wu, and M. Xiao, Phys. Rev. A **84**, 053820 (2011).
[26] D. Xuan Khoa, L. Van Doai, D. Hoai Son, and N. Huy Bang, J. Opt. Soc. Am. B **31**, 1330 (2014).
[27] M. Bajcsy, S. Hofferberth, V. Balic, T. Peyronel, M. Hafezi, A. S. Zibrov, V. Vuletic, and M. D. Lukin, Phys. Rev. Lett. **102**, 203902 (2009).
[28] J. Zhang, G. Hernandez, and Y. Zhu, Opt. Lett. **32**, 1317 (2007).
[29] N. Matsuda, R. Shimizu, Y. Mitsumori, H. Kosaka, and K. Edamatsu, Nat. Photon. **3**, 95 (2009).
[30] K. Bergmann, H. Theuer, and B. W. Shore, Rev. Mod. Phys. **70**, 1003 (1998).
[31] F. Vewinger, B. W. Shore, and K. Bergmann, in *Advances in Atomic, Molecular, and Optical Physics*, edited by E. Arimondo, P. R. Berman, and C. C. Lin (Elsevier, Amsterdam, 2010), Vol. 58, pp. 113–172.
[32] M. N. Kobrak and S. A. Rice, Phys. Rev. A **57**, 2885 (1998).
[33] J. Gong and S. A. Rice, J. Chem. Phys. **120**, 9984 (2004).
[34] M. Sugawara, Chem. Phys. Lett. **428**, 457 (2006).
[35] M. Mahmoudi, M. Sahrai, and M. A. Allahyari, Prog. Electromagn. Res. B **24**, 333 (2010).
[36] L. Ebrahimi Zohravi, R. Doostkam, S. M. Mousavi, and M. Mahmoudi, Prog. Electromagn. Res. M **25**, 1 (2012).
[37] M. O. Scully and M. S. Zubairy, *Quantum Optics* (Cambridge University Press, Cambridge, 1997).
[38] D. L. Campbell, G. Juzeliunas, and I. B. Spielman, Phys. Rev. A **84**, 025602 (2011).
[39] T. Volz, A. Reinhard, M. Winger, A. Badolato, K. J. Hennessy, E. L. Hu, and A. Imamoğlu, Nature Photonics **6**, 605 (2012).
[40] A. M. C. Dawes, L. llling, S. M. Clark, and D. J. Gauthier, Science **308**, 672 (2005).
[41] G. S. Agarwal and T. N. Dey, Phys. Rev. A **68**, 063816 (2003).
[42] L.-D. Zhang, Y. Jiang, R.-G. Wan, S.-C. Tian, B. Zhang, X.-J. Zhang, J.-Y. Gao, Y.-P. Niu, and S.-Q. Gong, J. Phys. B **44**, 135505 (2011).
[43] M. Shapiro, Z. Chen, and P. Brumer, Chem. Phys. **217**, 325 (1997).
[44] Z. Chen, M. Shapiro, and E Brumer, J. Chem. Phys. **98**, 8647 (1993).
[45] H.-R. Xia, C.-Y. Ye, and S.-Y. Zhu, Phys. Rev. Lett. **77**, 1032 (1996).